Pergamon

Int. J. Heat Mass Transfer. Vol. 41, Nos 4–5, pp. 681–689, 1998

Printed in Great Britain
0017-9310/98 $19.00+0.00

PII: S0017-9310(97)00229-9

Analytic analysis of heat loss from corners of buildings

D. TANG
Integrated Environmental Solutions Limited, 1 Atlantic Quay, Broomielaw, Glasgow G2 8JE, U.K.

and

G. S. SALUJA
School of Construction and Environment, University of Abertay Dundee, Bell Street, Dundee DD1 1HG, U.K.

(*Received* 4 *September* 1997)

Abstract—An analytic solution for the elliptic boundary value problem with irregular geometrical boundary region using Schwarz's alternating method is presented. The application of the solution addresses to the physical problems of temperature distribution and heat flux within homogeneous corners of buildings. A parametric analysis based on the general solution derives the concepts of "significant length" and "coefficient of equivalence" that can be used in engineering designs. © 1997 Published by Elsevier Science Ltd.

1. INTRODUCTION

Solution to the thermal condition problem of building structure concerns the classical boundary value problem of the transient, i.e. Fourier equation, or steady-state, i.e. Laplace equation under various boundary conditions. Typical analytic solutions are available for problems of regular geometrical boundaries by using tools like separation of variables and integral transforms [1, 2, 3]. Certain types of problems with irregular geometrical boundary may be solved using conformal mapping, co-ordinate transformation, or approximation techniques like Gerlerkin's method [4, 5]. Very often the problem becomes intractable even with a slight change in boundary conditions.

Thermal conduction is one of the major concerns in building design. For example, condensation causes structural damage to buildings and is also hazardous to the health of the occupants. Dampness occurs, most frequently, at a corner of two external walls and results in surface and interstitial condensation due to multi-dimensional heat transfer. At present, calculation methods provided by the engineering design Guides are derived from one-dimensional heat transfer theory [6, 7]. No method is provided to account for heat loss from corner and bridge structures.

While numerical methods are useful in solving heat transfer problems with irregular boundaries and non-linearity, issues remain that they give particular solutions to boundary value problems. The result can not be easily generalised to yield general solution [8]. Also discretisation and truncation errors of numerical methods are largely hidden. Careless use of numerical package would very often result in misleading results. To this end analytic solutions are needed as either the reference to validate the corresponding numerical methods or provide tools for engineering designs. Excellent examples may be found in Hassid [9] who solved the problem of two-dimensional multi-layered thermal bridge using a semi-discretisation technique; Krarti [10] who solved the problem of quasi-transient two-dimensional "slab-on-grade" type ground heat loss using complex variable and boundary profile estimation method, named as ITPE.

2. THE BOUNDARY VALUE PROBLEM

The boundary value problem for heat transfer in a homogeneous corner is shown in Fig. 1. Assuming that the heat flow and temperature distribution within the wall are two-dimensional; at distance further away from the corner longitudinal heat flow of the wall becomes negligible; temperatures of both inside and outside surfaces of the corner are subject to the boundary condition of the third-kind, i.e. dependent upon the rate of convective and conductive heat transfer of the corresponding sides.

Introducing the temperature excess, $\vartheta(x,y) = T(x,y) - T_0$, such that the reference temperature $\theta_1 = T_1 - T_0$, reference dimension, b, and defining to the following non-dimensional transformations:

$$\hat{\vartheta} = \frac{\vartheta}{\theta_1}; \quad \hat{x} = \frac{x}{b}; \quad \hat{y} = \frac{y}{b}; \quad \hat{a} = \frac{a}{b};$$

NOMENCLATURE

a, b	length and thickness of the wall, respectively [m]
Bi	Biot modulus
C_{eq}	coefficient of equivalence
F_n	discrete Fourier coefficients
H	rate of heat convection to conduction [m]
h	convective heat transfer coefficient of internal surface [W/m^2 K]
k	thermal conductivity [W/m K]
L_s	significant length [m]
q	heat flux [W/m]
T	temperature of wall [K]
U	U-value [W/m^2 K]
U^*	equivalent U-value [W/m^2 K]
x, y	space co-ordinates [m].

Greek symbols

$\alpha_s; \beta_{s,n}; \gamma_{s,n}; \delta_s$	coefficients of transformation
ε	ratio of internal to external convective heat transfer coefficients
ϑ	excess temperature [K]
θ_1	excess temperature of internal surface [K]
η_n	eigen-values.

Subscripts

n, s	indices of coefficient
0, 1	external and internal, respectively
I, II	regions.

Superscript

k	order of substitution.

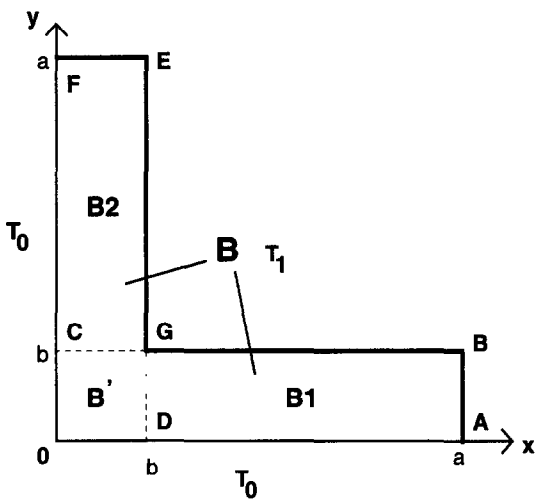

Fig. 1. Geometry of the boundary value problem.

$$Bi = \frac{h_0 b}{k}; \quad \varepsilon = \frac{h_1}{h_0}; \quad \hat{f}(x) = \frac{f(x)}{\theta_1}$$

The non-dimensional form of the boundary value problem of Fig. 1 is given in eqn (1).

$$\frac{\partial^2 \vartheta}{\partial x^2} + \frac{\partial^2 \vartheta}{\partial x^2} = 0 \quad x, y \in \text{ABGEF0}$$

$$-\frac{\partial \vartheta}{\partial x} + Bi\,\vartheta = 0 \quad x = 0, 0 \leqslant y \leqslant a$$

$$\frac{\partial \vartheta}{\partial x} + \varepsilon Bi\,\vartheta = \varepsilon Bi \quad x = 1; 1 \leqslant y \leqslant a$$

$$\frac{\partial \vartheta}{\partial x} = 0 \quad x = a; 0 \leqslant y \leqslant 1$$

$$\frac{\partial \vartheta}{\partial y} = 0 \quad y = a; 0 \leqslant x \leqslant 1$$

$$-\frac{\partial \vartheta}{\partial y} - Bi\,\vartheta = 0 \quad y = 0; 0 \leqslant x \leqslant a$$

$$\frac{\partial \vartheta}{\partial y} + \varepsilon Bi\,\vartheta = \varepsilon Bi \quad y = 1; 1 \leqslant x \leqslant a \qquad (1)$$

Note, in eqn (1) no circumflex is shown for the corresponding non-dimensional variables for clarity reason. Unless otherwise stated, the same format applies to the following text.

2.1. *The Schwarz's alternating method*

The concept of the Schwarz's alternating method is, in general, to subdivide the solution domain into regions where general solutions exist. Referring to Fig. 1, let the domain of the corner be region B enclosed by boundary ABGEF0; let B1 and B2 be the two sub-regions of domain B enclosed by boundary of ABC0 and DEF0, respectively; let B′ be the region of intersection between B1 and B2 and enclosed by DGC0, such that,

$$\text{B}' \subset \text{B1}; \quad \text{B}' \subset \text{B2}; \quad \text{B1} \cap \text{B2} = \text{B}';$$
$$\text{and} \quad \text{B1} \cup \text{B2} = \text{B} \qquad (2)$$

Provided that the general solutions exist for the regions of B1 and B2 based on piece-wise continuous boundary conditions, a solution over the domain B can be obtained by successive solution of the corresponding problems in the regions of B1 and B2. This is done by firstly assigning an arbitrary function on the border CG of B1 to construct a piece-wise continuous function. The solution obtained can then be used as the first approximation to construct the boundary

condition of B2. The successive solution progresses and thus generates a sequence of approximations to the sought solution, $\vartheta(x,y)$, over domain B, i.e.

$$\vartheta_1^{(1)}(x,y),\quad \vartheta_1^{(2)}(x,y),\ldots,\quad \vartheta_1^{(k)}(x,y),\ldots$$
$$\vartheta_2^{(2)}(x,y),\quad \vartheta_2^{(2)}(x,y),\ldots,\quad \vartheta_2^{(k)}(x,y),\ldots \qquad (3)$$

The proof of the existence and convergence of the sequence (3) to the general solution of the original boundary value problem of domain B may be found elsewhere [3].

2.2. *Solution of the boundary value problem*

To construct the solution of eqn (1), in the region of B1, assuming an arbitrary function on the border CG and the boundary condition of the third-kind on GB, a piece-wise continuous function $f_1(x)$ over the border BC is constructed. Similarly in B2, a piece-wise continuous function $f_2(y)$ over the border DE is constructed. This gives two well posed boundary value problems, as shown in eqns (4) and (5), respectively.

$$\frac{\partial^2\vartheta_1}{\partial x^2}+\frac{\partial^2\vartheta_1}{\partial y^2}=0 \quad x,y\in x,y\in \mathrm{ABC0}$$
$$\frac{\partial\vartheta_1(a,y)}{\partial x}=0 \quad 0\leqslant y\leqslant 1$$
$$-\frac{\partial\vartheta_1(0,y)}{\partial x}+Bi\,\vartheta_1(0,y)=0 \quad 0\leqslant y\leqslant 1$$
$$\frac{\partial\vartheta_1(x,0)}{\partial y}+Bi\,\vartheta_1(x,0)=0 \quad 0\leqslant x\leqslant a$$
$$\frac{\partial\vartheta_1(x,1)}{\partial y}+\varepsilon Bi\,\vartheta_1(x,1)=\varepsilon Bi f_1(x) \quad 0\leqslant x\leqslant a \qquad (4)$$

and

$$\frac{\partial^2\vartheta_{II}}{\partial x^2}+\frac{\partial^2\vartheta_{II}}{\partial y^2}=0 \quad x,y\in \mathrm{DEF0}$$
$$\frac{\partial\vartheta_{II}(x,a)}{\partial x}=0\leqslant x\leqslant 1$$
$$-\frac{\partial\vartheta_{II}(x,0)}{\partial x}+Bi\,\vartheta_{II}(x,0)=0 \quad 0\leqslant x\leqslant 1$$
$$-\frac{\partial\vartheta_{II}(0,y)}{\partial y}+Bi\,\vartheta_{II}(0,y)=0 \quad 0\leqslant y\leqslant a$$
$$\frac{\partial\vartheta_{II}(1,y)}{\partial y}+\varepsilon Bi\,\vartheta_{II}(1,y)=\varepsilon Bi f_2(y) \quad 0\leqslant y\leqslant a \qquad (5)$$

Since the two problems are symmetric along the line $y=x$, eqns (4) and (5) are mirror images of each other, i.e.

$$\vartheta_1(x,y)=\vartheta_{II}(y,x) \qquad (6)$$

Without losing generality, the solution will be demonstrated on solving eqn (4) for $\vartheta_1(x,y)$ in B1. The solution of $\vartheta_{II}(x,y)$ may be obtained using the mirror-image of $\vartheta_1(x,y)$.

Using the method of separation of variables [1], the eigen-values of eqn (4) can be found by solving the following transcendental equation:

$$\tan\eta_n a=\frac{Bi}{\eta_n} \quad (n=1,2,\ldots,n)$$

where $\eta_1<\eta_2<\eta_3<\cdots<\eta_n$ are the eigen-values.

The eigen-function is found as,

$$\vartheta_n(x,y)=\left(\cosh\eta_n y+\frac{Bi}{\eta_n}\sinh\eta_n y\right)\cos\eta_n(a-x)$$
$$(n=1,2,\ldots,n)$$

Assuming that the piece-wise continuous function $f_1(x)$ can be expanded into orthogonal series of $\cos\eta_n(a-x)$ (see Appendix 1), such that,

$$f_1(x)=\sum_{n=1}^{\infty}F_n\cos\eta_n(a-x) \qquad (7)$$

a trial solution to eqn (4) may be obtained in the form of,

$$\vartheta_1(x,y)=\sum_{n=1}^{\infty}\frac{F_n\left(\cosh\eta_n y+\dfrac{Bi}{\eta_n}\sinh\eta_n y\right)}{\left(\dfrac{\eta_n}{\varepsilon Bi}+\dfrac{Bi}{\eta_n}\right)\sinh\eta_n+\left(\dfrac{1}{\varepsilon}+1\right)\cosh\eta_n}\times\cos\eta_n(a-x) \qquad (8)$$

where F_n $(n=1,2,\ldots,n)$ are the coefficient sequence to be determined.

To construct the piece-wise continuous function on the border of BC, define

$$f_1(x)=\varepsilon Bi\begin{cases}\dfrac{1}{\varepsilon Bi}\dfrac{\partial\vartheta_1(x,y)}{\partial y}+\vartheta_{II}(x,y)\Big|_{y=1} & 0\leqslant x\leqslant 1\\ 1 & 1\leqslant x\leqslant a\end{cases} \qquad (9)$$

Substituting the trial solution, i.e. eqn (8), into the boundary condition of the third-kind at $y=b$,

$$\frac{\partial\vartheta_1(x,1)}{\partial y}+\varepsilon Bi\,\vartheta_1(x,1)=\varepsilon Bi f_1(x) \qquad (10)$$

multiplying each term of eqn (10) by $\cos\eta_s(a-x)$ and integrating over the interval of $[0,a]$, re-arranging all the terms and after the kth successive substitution, the formulation of the solution sequence of F_n yields:

$$\left(a_s+\frac{1}{\varepsilon Bi}\beta_{s,s}-\gamma_{s,s}\right)F_s^{(k)}=\sum_{\substack{n=1\\ n\neq s}}^{M}\gamma_{s,n}F_n^{(k-1)}-\frac{1}{\varepsilon Bi}\sum_{\substack{n=1\\ n\neq s}}^{M}\beta_{s,n}F_n^{(k-1)}+\delta_s$$
$$(s=1,2,\ldots,M) \qquad (11)$$

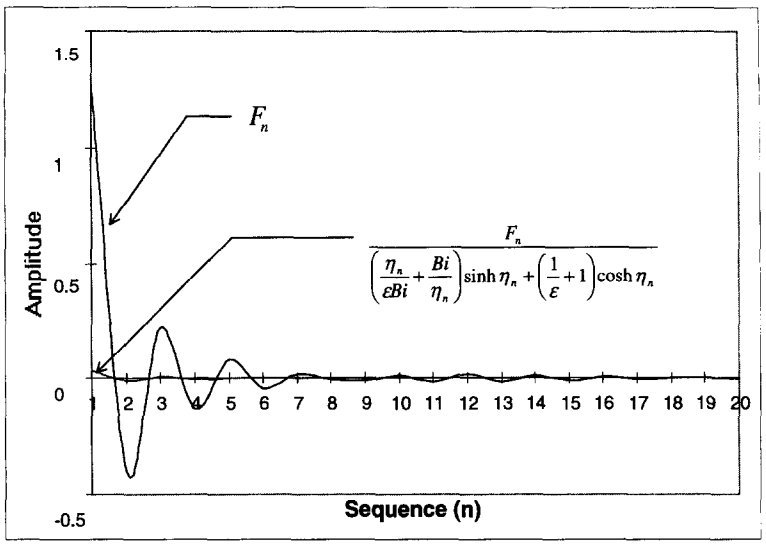

Fig. 2. The sequences of coefficients and coefficient-group.

where, M is the upper limit for the truncation of infinitive summation. As the infinitive summations are convergent, the lower limit of M is determined such that the increase of which does not cause significant changes in coefficient sequence F_n.

The formulations of coefficients $\alpha_i; \beta_{s,n}; \gamma_{s,n}; \delta_s$ are given in Appendix 2.

The initial values of the coefficient sequence F_n $(n = 1, 2, \ldots, M)$ are obtained by assuming the following continuous boundary condition over the entire border of BC, i.e.

$$\frac{\partial \vartheta_1(x,1)}{\partial y} + \varepsilon\, Bi\, \vartheta_1(x,1) = \varepsilon\, Bi \cdot 1 \tag{12}$$

Successive computation of eqn (11) results in the following coefficient sequences:

$$\begin{aligned} &F_1^{(1)}(x,y), \quad F_1^{(2)}(x,y), \ldots, \quad F_1^{(k)}(x,y), \ldots \\ &F_2^{(2)}(x,y), \quad F_2^{(2)}(x,y), \ldots, \quad F_2^{(k)}(x,y), \ldots \end{aligned} \tag{13}$$

It has been proved that the sequences of eqn (13) are uniformly converging and therefore solutions of $\vartheta_1(x,y)$ and $\vartheta_{II}(x,y)$ are convergent. In practice, the successive substitution process stops after satisfying the following convergence criterion:

$$\frac{\|\mathbf{F}^{(k)} - \mathbf{F}^{(k-1)}\|}{\|\mathbf{F}^{(k)}\|} \leqslant \sigma \tag{14}$$

Figure 2 shows the sequence of coefficient F_n obtained after 22 successive substitutions based on the criterion of $\sigma = 10^{-7}$. It can be seen that coefficient seqeuence F_n $(n = 1, 2, \ldots, M)$ converges uniformly and in particular, coefficient group

$$\frac{F_n}{\left(\frac{\eta_n}{\varepsilon\, Bi} + \frac{Bi}{\eta_n}\right)\sinh\eta_n + \left(\frac{1}{\varepsilon}+1\right)\cosh\eta_n}$$

diminishes after $n > 20$

3. PARAMETRIC ANALYSIS

3.1. *Error estimation*

By using eqn (11) incorporating the coefficient sequence of F_n $(n = 1, 2, \ldots, M)$ shown in Fig. 2, the temperature field within domain B1 can be found.

Figure 3 shows the non-dimensional temperature contours of the region of B1 for up to the length of $L/b = 3.0$. The prediction of Fig. 3 was based upon: $\varepsilon = 0.5$; $Bi = 10$; $\theta_1 = 1$ and using 100 coefficients.

To evaluate the accuracy of the prediction, Table 1 shows the non-dimensional temperature distribution within the symmetric region of B′. The maximum non-symmetry error with reference to the dissector, $y = x$, is found by,

$$e = \max|\vartheta_1(x,y) - \vartheta_1(y,x)| \leqslant 0.0008$$

It is possible to increase the accuracy of non-symmetry by further reducing the convergence criterion σ of eqn (14).

3.2. *Comparison of numerical prediction*

Comparison to the results obtained using numerical prediction has been made [11]. The numerical prediction was based on a five-point central difference scheme with second-order accuracy, i.e.

$$\frac{\vartheta_{x+\Delta x,y} - 2\vartheta_{x,y} + \vartheta_{x-\Delta x,y}}{\Delta x^2} + \frac{\vartheta_{x,y+\Delta y} - 2\vartheta_{x,y} + \vartheta_{x,y-\Delta y}}{\Delta y^2} = 0 \tag{15}$$

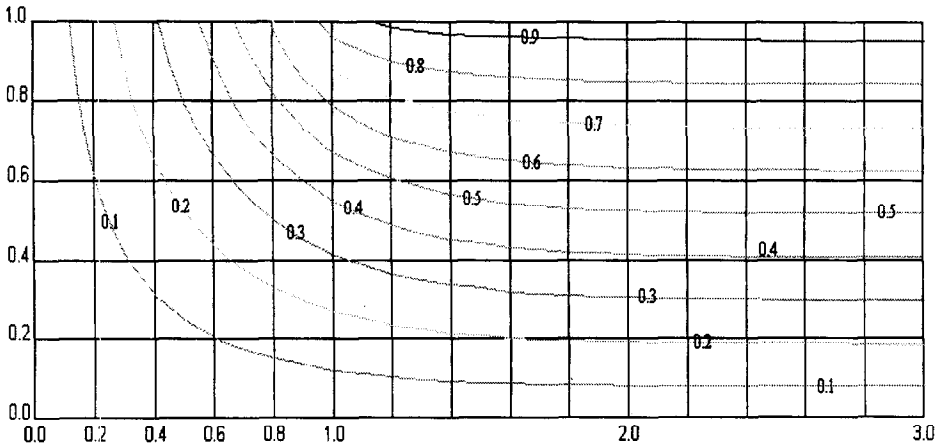

Fig. 3. Temperature contour of the corner.

Table 1. Non-dimensional temperature distribution within region B′

x, y	0	0.2	0.4	0.6	0.8	1.0
0	0.00066	0.00487	0.00906	0.01317	0.01703	0.01965
0.2	0.00487	0.03603	0.06717	0.0978	0.12676	0.15164
0.4	0.00906	0.06717	0.12564	0.18397	0.23997	0.28898
0.6	0.01317	0.0978	0.18397	0.27206	0.35962	0.4379
0.8	0.01703	0.12677	0.23998	0.35962	0.48704	0.61005
1.0	0.02043	0.15226	0.28944	0.43817	0.60999	0.84973

Equation (15) represents a numerical solution to the original partial differential problem with a certain accuracy as determined by the truncation and round-off errors.

Using Taylor expansion, $\vartheta_{x\pm\Delta x,y}$; $\vartheta_{x,y\pm\Delta y}$ can be represented as follows

$$\vartheta_{x\pm\Delta x,y} = \vartheta_{x,y} \pm \left(\frac{\partial\vartheta}{\partial x}\right)\Delta x + \frac{1}{2!}\left(\frac{\partial^2\vartheta}{\partial x^2}\right)\Delta x^2 \ldots$$

$$\vartheta_{x,y\pm\Delta y} = \vartheta_{x,y} \pm \left(\frac{\partial\vartheta}{\partial y}\right)\Delta y + \frac{1}{2!}\left(\frac{\partial^2\vartheta}{\partial y^2}\right)\Delta y^2 \ldots \quad (16)$$

Substitute expansion (16) into eqn (15) and rearrange the terms, the truncation error of eqn (15) gives,

$$\frac{\partial^2\vartheta}{\partial x^2} + \frac{\partial^2\vartheta}{\partial y^2} = R(x,y) \quad (17)$$

where,

$$R(x,y) = -\frac{2}{4!}\left[\left(\frac{\partial^4\vartheta}{\partial x^4}\right)\Delta x^2 + \left(\frac{\partial^4\vartheta}{\partial y^4}\right)\Delta y^2\right] + O(\Delta x^4, \Delta y^4)$$

which is the truncation error associated with the finite difference discretisation. Clearly, the truncation error is in the order of $O(\Delta x^2, \Delta y^2)$ and negative definite.

It follows that when the numerical form of the boundary-value problem, i.e. eqn (15), is being solved, it is, in reality a Poisson equation, i.e. eqn (17), being solved instead of the original Laplace equation. This gives a clear indication to the behaviour of the results to be expected from the numerical method. The truncation error, $R(x,y)$ acts as a source term. As being negative, it may be viewed as an "artificial heat sink" which is purely numerical origin and has no physical significance.

Inspection of eqn (17) reveals that the intensity of the "artificial heat sink" diminishes progressively when the size of the numerical cell reduces progressively and the numerical prediction approaches progressively towards the analytic solution.

Figure 4 shows the deviations between the analytical and numerical prediction referring to the location of the inside corner denoted by $\vartheta(1,1)$, in which a uniform spatial step, i.e. $\Delta x \equiv \Delta y \equiv \Delta h$, is used for the ease of demonstration.

The analytic solution may be useful as a tool to supplement the results obtained using transient one-dimensional conduction simulation packages using finite difference or response function methods, e.g.

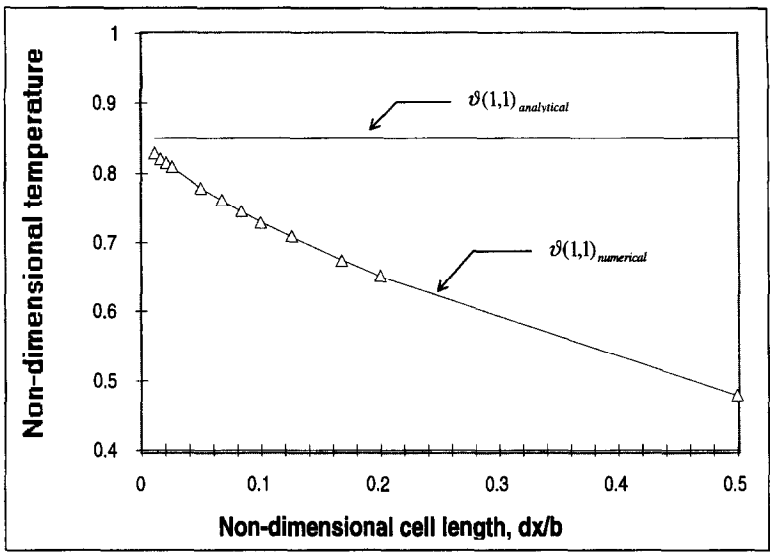

Fig. 4. Comparison of analytic and numerical predictions.

ESP, TRNSYS, to generate two-dimensional temperature fields of the corner for the assessment of condensation risk.

3.2. *The significant length*

The significant length is defined as the distance L_s from the corner beyond which the heat flow parallel to the wall becomes negligible, i.e.

$$\left.\frac{\partial\vartheta(x,y)}{\partial x}\right|_{x\geqslant L_s}\approx 0.$$

Let e be the minimal allowable error, the corresponding distance of L_s may be found as follows:

$$\left.\frac{\partial\vartheta_1(x,b/2)}{\partial x}\right|_{x=L_s}= \sum_{n=1}^{\infty}\frac{F_n\eta_n\left[\cosh\frac{\eta_n}{2}+\frac{Bi}{\eta_n}\sinh\frac{\eta_n}{2}\right]\sin\eta_n(a-L_s)}{\left(\frac{\eta_n}{\varepsilon Bi}+\frac{Bi}{\eta_n}\right)\sinh\eta_n+\left(\frac{1}{\varepsilon}+1\right)\cosh\eta_n}\leqslant e \quad (18)$$

For example, for an allowable error of $e < 0.001$, the corresponding significant length of $L_s > 3.098$ is found. For $x \geqslant L_s = 3.0$, the heat flow may be considered one-dimensional based on an allowable error of 0.0013. Fig. 5 shows the characteristics of the significant length.

3.3. *The equivalent U-value and the coefficient of equivalence*

In engineering design, the heat loss of an external wall is usually calculated based on the internal floor length of the wall. The local heat flux of an inside surface can be calculated by using eqn (8), which gives:

$$q(x,y)\Big|_{y=1}=k\left.\frac{\partial\vartheta(x,y)}{\partial y}\right|_{y=1}= k\theta_1\sum_{n=1}^{M}\frac{F_n\eta_n\left(\sinh\eta_n+\frac{Bi}{\eta_n}\cosh\eta_n\right)\cos\eta_n(a-x)}{\left(\frac{\eta_n}{\varepsilon Bi}+\frac{Bi}{\eta_n}\right)\sinh\eta_n+\left(\frac{1}{\varepsilon}+1\right)\cosh\eta_n} \quad (19)$$

The total heat loss over the internal surface with a length of X and unit height can be found by,

$$Q_X=\int_1^X q(x,1)\,dx \quad (20)$$

Introducing the significant length such that for all $x > L_s$, $q(x,1)|_{x>L_s} = \text{const.}$ eqn (20) becomes,

$$Q_X=\int_1^{L_s} q(x,1)\,dx+U\theta_1(x-L_s) \quad (21)$$

Let U^* be the equivalent U-value, such that,

$$U^*\theta_1(L_s-1)=\int_1^{L_s} q(x,1)\,dx \quad (22)$$

Equation (21) becomes,

$$Q_X=U^*\theta_1(L_s-1)+U\theta_1(X-L_s) \quad (23)$$

Let C_{eq} be the coefficient of equivalence, such that

$$C_{eq}=\frac{U^*}{U}\quad\text{or}\quad U^*=C_{eq}U$$

and eqn (23) becomes,

$$Q_X=\left[1+(C_{eq}-1)\frac{L_s-1}{X-1}\right]U\theta_1(L_s-1) \quad (24)$$

Assuming for $L_s = 3.0$, let $L = X-1$ be the length

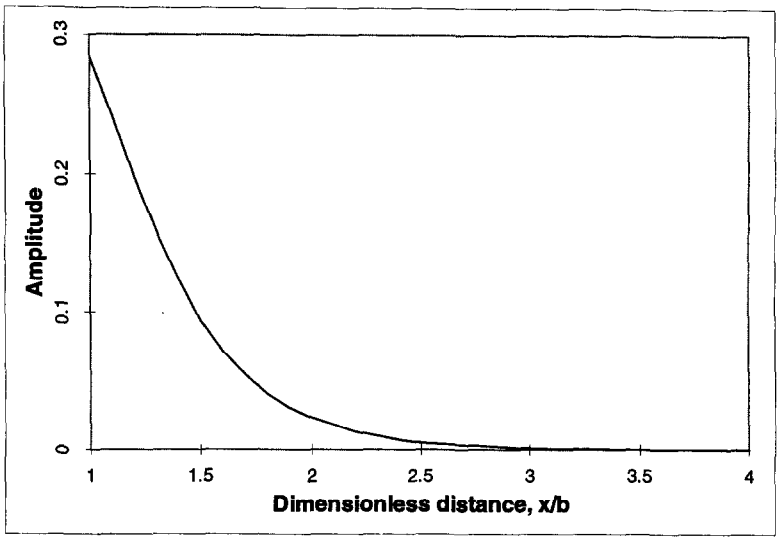

Fig. 5. The significant length.

of the wall measured from the internal corner and height of the wall W, eqn (24) becomes,

$$Q_x = \left[1 + (C_{eq} - 1)\frac{2}{L}\right] U\theta_1 LW \tag{25}$$

It can be seen from eqn (25) that the "corner effect" diminishes and the heat flow approaches one-dimensional pattern when the length of the wall, L, increases.

The coefficient of equivalence, C_{eq}, may be calculated based on eqn (22), i.e.

$$C_{eq} = \frac{1}{2}\left[\frac{1}{Bi}\left(1+\frac{1}{\varepsilon}\right)+1\right] F_n\left(\sinh\eta_n + \frac{Bi}{\eta_n}\cosh\eta_n\right) \times \sum_{n=1}^{M} \frac{[\sin\eta_n(a-1) - \sin\eta_n(a-3)]}{\left(\frac{\eta_n}{\varepsilon\, Bi} + \frac{Bi}{\eta_n}\right)\sinh\eta_n + \left(\frac{1}{\varepsilon}+1\right)\cosh\eta_n} \tag{26}$$

Figure 6 shows the results of C_{eq} with reference to Biot modulus and ratio ε obtained using eqn (26).

Example: To calculate the heat loss from a one-sided corner of multi-layered wall with unit height and various length, external convective heat transfer coefficient $h_0 = 16.0$ W/m^2 K and internal convective heat transfer coefficient of $h_1 = 8.0$ W/m^2 K, the structure of wall is given as follows:

Layer	Thickness (mm)	Conductivity (W/mK)	Resistance (m^2 K/W)
Brick	105	0.84	0.125
Cavity	75	—	0.18
Insulation	50	0.03	1.48
Brick	105	0.84	0.125
Plaster	15	0.16	0.09

Based on the above a U-value of 0.457 W/m^2 K is found. An average conductivity of $k = 0.175$ W/m K is derived based on

$$\sum_i l_i \Big/ \sum_i R_i.$$

To calculate the two dimensional heat loss, firstly find Biot modulus $Bi = 32.0$ and $\varepsilon = 0.5$. The coefficient of equivalence is obtained from Fig. 6, as $C_{eq} = 1.124$. Heat loss can then be calculated using eqn (25).

As a comparison, heat losses calculated based on the analytic formula of eqn (20), simplified formula of eqn (25) and one-dimensional U-value are given in Table 2. The relative error is based on $(Q_{theoretical} - Q_{1d})/Q_{1d}$. For two-sided corner wall, the error could be doubled.

3.4. *Comparison with approximate method*

Approximate methods, also known as the textbook methods, derived using the techniques of conformal mapping, graphic method, etc. are available as an effective way of producing estimation for the total heat transfer rate through an irregular geometry. These methods are mainly derived based on the boundary condition of the first-kind by which the surface temperature are known. The conduction shape factor method is used here as a further example for the comparison exercise.

Using the conduction shape factor method, the rate of heat transfer may be written as

$$q = k \cdot S \cdot \Delta T \tag{27}$$

where

k thermal conductivity.
S conduction shape factor.
ΔT temperature difference of inner and outer surface.

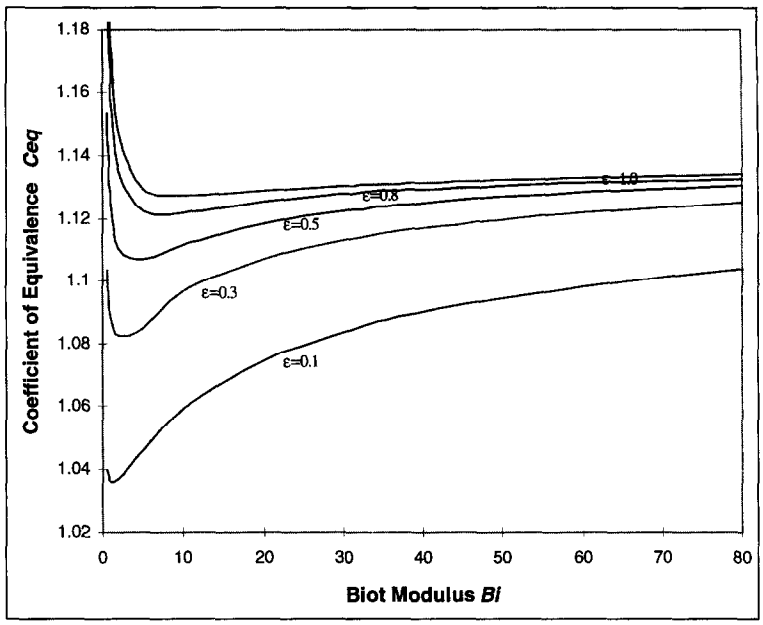

Fig. 6. The coefficient of equivalence of U-value.

Table 2. The comparison of calculations of heat losses

L/b	$Q_{\text{theoretical}}/b$ (W/m)	$Q_{\text{simplified}}/b$ (W/m)	Q_{1d}/b (W/m)	Error (%)
2	0.571	0.571	0.457	24.945
3	1.031	1.028	0.914	12.801
5	1.946	1.942	1.828	6.455
6	2.403	2.399	2.280	5.395
8	3.317	3.313	3.194	3.851
10	4.231	4.227	4.109	2.969

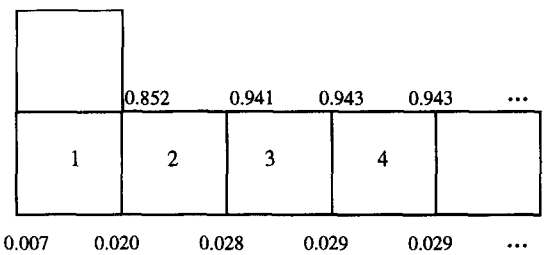

Fig. 7. Surface temperature field of the corner.

For conduction through two plane sections and the edge section of two walls of thermal conductivity k and uniform inner and outer surface temperature, the conduction shape factor, S is given by, based on unit width of the wall [12];

$$S = \frac{2L}{b} + 0.54 \tag{28}$$

For one-sided corner wall, after arrangement, eqn (28) becomes,

$$q = k\left(\frac{L}{b} + 0.27\right)\Delta T \tag{29}$$

Again here ΔT is the surface temperature difference.

To use eqn (29), one has to find the two-dimensional temperature distribution on the inner and outer surface of the corner wall. Here, the two-dimensional surface temperature field is found using the analytical method, i.e. eqn (8) based on the properties used in the previous example. Figure 7 shows the temperature field of the inner and outer surface of the corner.

To calculate the rates of heat transfer over various lengths of the wall using the conduction shape factor method, the mean surface temperature difference over a given length has to be found. This is done by taking an average value of the participating nodal temperatures over the corresponding length, which gives, according to Fig. 7,

Sections	1–2	1–3	1–5	1–6	1–8	1–10
ΔT	0.880	0.891	0.902	0.903	0.906	0.908

The heat losses from the one-sided corner are then calculated using eqn (29), i.e.

L/b	2	3	5	6	8	10
Q/b (W/m)	0.576	1.036	1.938	2.393	3.301	4.209

It can be seen that on average the results obtained using the conduction shape factor method are close to the exact solution, second to the simplified method and better than the U-value method. Clearly the question remains that how the surface temperatures are

obtained. The selection of surface temperatures is critical in using this method. In practice, it is difficult to find the correct surface temperatures of a wall prior to calculate the heat losses based on knowing the internal and external air temperatures. Theoretically, boundary value problems of boundary condition of the first and third kinds are two distinctive problems, they require different solution techniques and each serves its own domain of applications.

4. CONCLUSION

A general solution for the elliptic boundary value problem of two-dimensional corner with convective boundary condition using the Schwarz's alternating method is presented. The solution may be used to predict the temperature distribution within a two-dimensional corner of building. The accuracy of the general solution has been examined and comparison to the numerical prediction has been analysed. The concept of the "significant length" has been derived which indicates the influence of the two-dimensional corner thermal bridge effect. A simplified while accurate formulation of the equivalent U-value is derived. Example has been demonstrated for the calculation of heat loss in engineering design.

REFERENCES

1. Carslaw, H. S. and Jaeger, J. C., *Conduction of Heat in Solid*. Clarendon Press, Oxford, 1959.
2. Churchill, R. V. and Brown, J. W., *Fourier Series and Boundary Value Problems*. McGraw-Hill, 1987.
3. Kantorovich, L. V. and Krylov, V. I., *Approximate Methods for High Analysis*. Interscience, 1964.
4. Churchill, R. V., *Complex Variables and Applications*. McGraw-Hill, 1984.
5. Ozisik, M. N., *Boundary Value Problems of Heat Conduction*, International Textbook Co., 1968.
6. ASHRAE, *ASHRAE Handbook of Fundamental*: Ch. 20 Thermal insulation and vapour retarders, 1993.
7. CIBSE, *CIBSE Guide*, Section A3: Thermal properties of building structures, 1988.
8. Oreszczyn, T., Cold bridge at corners: surface temperature and condensation risk. In *Building Serv. Eng. Res. Technol.*, 1988, **9**(4), pp. 167–175.
9. Hassid, S., Thermal bridge across multi-layer wall: a simplified approach. In *Building and Environment*, Vol. 24, no. 3, pp. 259–264, 1989.
10. Krarti, M., Time varying heat transfer from slab-on-grade floor with vertical insulation. *Building and Environment*, Vol. 29, No. 1, pp. 55–61, 1994.
11. Tang, D., Numerical prediction of temperature in building structures: sser's manual of CORNER1. *CES&B Report*, University of Abertay Dundee, 1993.
12. Krieth, F., *Principles of Heat Transfer*, Harper & Row, 1976, pp. 93.

APPENDIX 1

Since the eigen-values of kernel sequence $\cos\eta_n(a-x)$, $(n = 1, 2, \ldots, n)$ are not integers, the sequence is not Fourier series, However, it may be proved that if such expansion satisfies the following orthogonal conditions, i.e.

1. the kernel functions can be integrated;
2. the kernel functions satisfy the orthogonal condition, i.e. for $X_n = \cos\eta_n(a-x)$, $(n = 1, 2, \ldots)$

$$\int_0^a X_n X_m \, dx = \begin{cases} 0 & n \neq m \\ F_n & n = m \end{cases}$$

the expansion is orthogonal.

APPENDIX 2

Formulations of coefficients used in eqn (11) are listed as follows:

$$\alpha_s = \phi_s\left(\frac{a}{2} + \frac{1}{4\eta_s}\sin 2\eta_s a\right) \tag{A1}$$

$$\beta_{s,n} = \psi_n \begin{cases} \dfrac{\sin(\eta_n+\eta_s)(a-1)}{2(\eta_n+\eta_s)} + \dfrac{\sin(\eta_n-\eta_s)(a-1)}{2(\eta_n-\eta_s)} & (n \neq s) \\ \dfrac{a-1}{2} + \dfrac{1}{4\eta_s}\sin\eta_s(a-1) & (n = s) \end{cases} \tag{A2}$$

$$\gamma_{s,n} = \omega_n \frac{1}{\eta_n^2+\eta_s^2}\left[\eta_s\cos\eta_s(a-1)\left(\sinh\eta_n + \frac{Bi}{\eta_n}\cosh\eta_n\right) - \eta_s\sin\eta_s(a-1)\left(\cosh\eta_n + \frac{Bi}{\eta_n}\sinh\eta_n\right)\right] \tag{A3}$$

$$\delta_s = \frac{1}{\eta_s}\sin\eta_s(a-1) \quad (s = 1, 2, \ldots, M; n = 1, 2, \ldots, M) \tag{A4}$$

in which

$$\phi_n = \frac{\cosh\eta_n + \dfrac{Bi}{\eta_n}\sinh\eta_n}{\left(\dfrac{\eta_n}{\varepsilon\, Bi} + \dfrac{Bi}{\eta_n}\right)\sinh\eta_n + \left(\dfrac{1}{\varepsilon}+1\right)\cosh\eta_n} \tag{A5}$$

$$\psi_n = \frac{\eta_n\sinh\eta_s + Bi\cosh\eta_n}{\left(\dfrac{\eta_n}{\varepsilon\, Bi} + \dfrac{Bi}{\eta_n}\right)\sinh\eta_n + \left(\dfrac{1}{\varepsilon}+1\right)\cosh\eta_n} \tag{A6}$$

$$\omega_n = \frac{\cos\eta_n(a-1)}{\left(\dfrac{\eta_n}{\varepsilon\, Bi} + \dfrac{Bi}{\eta_n}\right)\sinh\eta_n + \left(\dfrac{1}{\varepsilon}+1\right)\cosh\eta_n} \quad (n = 1, 2, \ldots, M) \tag{A7}$$